Stochastic Environmental Research and Risk Assessment (2024) 38:1721–1739
https://doi.org/10.1007/s00477-023-02651-6

ORIGINAL PAPER

Elevational trends of land surface temperature in the Alborz Mountains within the context of global warming

Gholamreza Roshan[1] · Reza Sarli[2] · Stefan W. Grab[3] · Vahid Nasiri[2] · Jaroslaw Socha[2]

Accepted: 17 December 2023 / Published online: 24 January 2024

Abstract
Much recent scientific focus has been on the impact of climate change on human and natural environments. However, a particular research gap that we address is evaluating the effect of global warming on land surface temperatures across different spatial contexts, such as elevation, in mountain regions. Our aim is to establish the effect of global warming on daytime land surface temperatures at various elevations and slope aspects of the central Alborz Mountains in northern Iran. The land surface temperature (LST) component is extracted from MODIS Terra sensor satellite images for the period 2001–2021 on a monthly basis (240 images were used). Results indicated that increasing surface temperature trends are more pronounced than decreasing trends. Significant increasing surface temperature trends are observed for the months of January through December and June through July. In contrast, October records significant decreasing trends across all study areas and geographic domains. Rates of surface temperature increases are lower in the northern zones compared to the southern zones of the Central Alborz, for elevations ranging from 1500 to 4000 m above sea level. A key finding is that global warming has increased surface temperatures on both the northern and southern aspects of the western and mid regions of the Central Alborz Mountains, while no changes are noted for the eastern region.

Keywords Global warming · Temperature gradient · Elevation · Alborz Mountains

1 Introduction

Land surface temperature (LST) plays a crucial role in global change studies, particularly in the estimation of radiation values and the environmental heat balance for climate modeling (Kayet et al. 2016). Usually, seasonal and interannual fluctuations in air temperature are smaller than those at the Earth's surface. (Oko et al. 2006; do Nascimento et al. 2022). Changes in the daily cycle of LSTs are also strongly influenced by surface characteristics and local environmental conditions such as air flow and insolation at the ground surface (Dutta et al. 2022). Given that meteorological parameters measured by synoptic stations are usually set at ~ 1.5 m above the ground surface and are highly location-specific, such data are unsuitable for generalization across a regional scale, and especially so where the topography is diverse (Dowling, et al., 2022). This challenge is surmounted by leveraging remotely sensed thermal data captured within the thermal infrared portion of the electromagnetic spectrum. In this approach, the thermal emissions from the Earth's surface, which directly correspond to land surface temperature, are detected and measured using sensors sensitive to thermal infrared radiation. This technique allows for the collection of valuable temperature data across vast areas without the limitations posed by ground-based measurements (Sahani 2021).

Global surface temperatures have surged to unprecedented record highs in recent decades, with consequential stress and challenges for societies and environments worldwide (Briscoe et al., 2023). Global warming rates during the twentieth century have been widely documented, but are even more pronounced and concerning during the first 2 decades of the twenty-first century (Wang et al. 2022). For instance, it is estimated that the global mean surface

✉ Gholamreza Roshan
ghr.roshan@gu.ac.ir

1 Department of Geography, Golestan University, Shahid Beheshti, Gorgan, Iran

2 Department of Forest Resources Management, Faculty of Forestry, University of Agriculture in Krakow, Krakow, Poland

3 School of Geography, Archaeology and Environmental Studies, University of the Witwatersrand, Johannesburg, South Africa

air temperature has increased by 1.09 °C over the last decade (2011–2020), relative to the period 1850–1900 (IPCC, 2014; Chen et al. 2022a, b). However, at the global scale, such warming rates may be highly variable in space and time, with some areas even experiencing cooling or relatively stable climate conditions during the past few decades (Estrada et al. 2021). In addition, the northern hemisphere has warmed more than twice as fast as the southern hemisphere (Wu et al. 2023). Understanding the spatial contexts of these temperature variations holds considerable importance given their profound implications for regional hydrological and environmental processes, such as permafrost thaw (Ma et al. 2023), ice melt (Ivanov 2023), slope stability (Thomas et al. 2023), and the frequency and intensity of tropical storms (Kaur et al. 2023). Nevertheless, accurately projecting future temperature changes remains a formidable challenge, particularly when considering finer spatial scales (Park et al., 2023).

There is a general agreement in the literature that regions most strongly impacted by warming trends are terrestrial areas at high latitude or elevation (Overland et al. 2018; Thompson et al. 2021). Mountain regions are particularly sensitive to global warming and in several cases high mountain environments have warmed more rapidly than in adjacent lower elevation areas (e.g., Mountain Research Initiative EDW Working Group, 2015). This has important implications for mountain bio-diversity, water security and landscapes (e.g., Körner 2003). Warming at high elevations has also impacted the cryosphere (i.e., permafrost, glaciers, snow cover), with in many cases glaciers rapidly retreating or disappearing (e.g., Sommer et al. 2020), permafrost thawing and causing slope instability (e.g., Swanson 2021), and snow packs declining in their annual longevity (e.g., Huning and Aghakouchak 2018). Given that snow has important thermal regulatory control on the substrate (soil, rock) through its insulating properties, humidity and moisture, and reflective properties on insolation, changes in snowpack thickness and longevity have direct implications on soil temperatures. Such climate warming related changes in mountain regions have knock-on effects on biosystems, and very importantly, on water availability. Mountains are oftentimes referred to as "Water Towers" (e.g., Hill 2013) given their source of regulated and reliable water to surrounding drier regions (Viviroli and Weingartner 2004). To this end, changes in mountain water storage (as glaciers and snowpacks) are likely to impact future water availability for human consumption, irrigation and power generation.

Prior investigations into climate-related changes in Iranian mountain regions have provided valuable insights. Using oak tree ring data, Azizi et al. (2013) reconstructed precipitation patterns and trends for the central Zagros Mountains, dating back to A.D. 1840. Tree-ring data have also been used to establish ecological implications of recent warming on oak forest health in the Zagros Mountains (Arsalani et al. 2022). Detection and attribution of seasonal climate variability has also been considered for lower elevations (hillsides) of the Central Alborz Mountains (Naseri et al. 2021). In contrast, future climate projections with ensemble species distribution modeling for potential habitat shifts of *Salvia hydrangea* have been considered for the Central Zagros Mountains (Ardestani and Ghahfarrokhi 2021). Collectively, these studies span a wide spectrum of climate-related investigations for the Zagros and Alborz Mounains, ranging from historical precipitation trends to future habitat projections, climatic attribution, and ecological responses. Given that most lower elevation regions surrounding high mountains in Iran are climatologically and hydrologically semi-arid to arid, any climate change related alteration to reducing mountain water resources has critical implications for agriculture and society (Asakereh and Ashrafi 2023). To ensure appropriate planning and preparation for future climate-water scenarios in Iran, it is essential to undertake downscaled approaches to establish region-specific changes in temperature and hydrology. About 16% of Iran's population, primarily those living in the provinces of Alborz and Tehran, directly depend on water resources originating from the Central Alborz Mountains. Given climate warming and associated impacts in these mountains, water scarcity has become an acute concern to the region (Daneshvar et al. 2019; Vaghefi et al. 2019; Nagha and Farid Mojtahedi 2020). To this end, and in an attempt to establish potential spatial differences in environmental warming across this mountain landscape, our aim is to investigate spatial–temporal patterns of surface temperature changes during the last 2 decades.

2 Materials and methods

2.1 Study area

The Central Alborz Mountains, situated in northern Iran (between 35° 50′ to 36° 40′ N and 50°50′ to 52°50′ E), constitute Iran's highest mountain range. They feature a dramatic elevation change, ranging from − 40 m above sea level near the Caspian Sea to a towering 5,671-m a.s.l. at the summit of Mount Damavand (Nasiri et al., 2022). The northern Central Alborz Mountains receive varying precipitation levels (500–1500 mm per year), depending on elevation. These areas are mainly covered by Hyrcanian forests, extending up to around 2850 a.s.l (Noroozi et al., 2008; Karimi et al. 2015). The climate shifts from a humid-warm-temperate on the northern side to a continental-semiarid climate on the southern side, characterized by noticeable summer drought (Foroozan et al. 2020). However, at high elevation, the climate remains Mediterranean-type, with considerable snowfall during late autumn, winter and early spring seasons. In line with our research objectives, the Central Alborz is categorized into three sub-regions: the Eastern, Middle, and Western Alborz (Fig. 1). Additionally, each of these sub-regions is further divided into the northern (N) and southern (S) aspects of the mountain range. Elevations range from 1000 to 4000 m a.s.l., as indicated in Table 1. For defining elevation gradients, we'll refer to each 500 m elevation zone using its uppermost value (e.g., 1000-1500 m a.s.l. will be denoted as 1500 m a.s.l.). LST changes are determined by elevation across different landscape components. For specific area coverage (in hectares) and mean slope gradients (in degrees), please see Table 1.

2.2 Land surface temperature extraction

To extract monthly Land Surface Temperature (LST), we employed the Moderate Resolution Imaging Spectroradiometer (MODIS) satellite MOD11A2.061 Terra LST product, which operates at a daily time scale and offers a spatial resolution of 1 km. We generated an image collection considering all the MOD11A2.061 images for the period of 2001–2021. Prior to extracting the LST time series, quality bit masks were employed to filter out low-quality images. Only the pixels with good quality were retained, eliminating the need for examining more detailed quality indicators. Based on resulted LST pixels, we calculated the mean monthly LST for each study site. In this regard, we utilized the capabilities of the Google Earth Engine (GEE) cloud

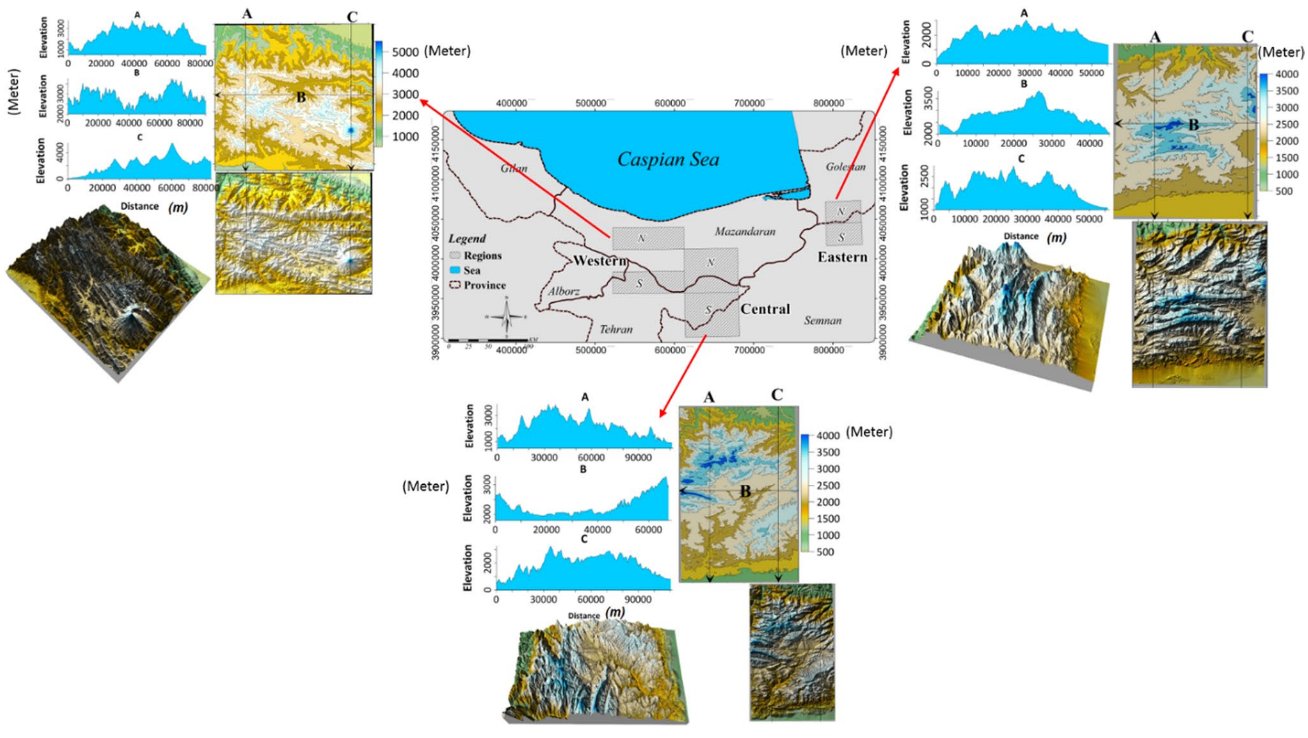

Fig. 1 Geographical location of key study regions including the Western, Middle and Eastern Central Alborz Mountains. Height profile changes are also given for each of the study regions

Table 1 Area (hectares) and mean slope gradient (degrees) for elevation classes on north (N) and south (S) aspects of the three study regions

Elevation (m a.s.l.)	West				Middle				East			
	N	slope	S	slope	N	Slope	S	slope	N	slope	S	slope
1000–1500	46,357.2	21.98	9522	6.27	42,793	23.20	54,109.6	11.01	10,495.6	23.25	30,714.4	4.02
1500–2000	65,248.2	22.06	40,196.9	14.65	50,752.6	24.06	83,661.1	19.29	17,093.5	25.91	29,522.1	9.51
2000–2500	41,604.9	22.99	68,367.7	21.03	95,350.3	20.60	139,257.2	19.54	46,661.5	21.53	39,598	18.29
2500–3000	24,896.1	24.97	85,805.7	24.22	78,694.7	20.74	59,469.8	18.63	34,100.9	20.66	16,094.7	21.93
3000–3500	10,986	25.79	36,339.1	25.22	50,470.2	22.83	6697.5	19.89	6546.7	22.31	8136.5	26.09
3500- 4000	1124.5	26.28	7484.8	26.15	9869.2	23.26	653.1	24.66	1402.4	26.55	453.2	28.01

computing platform. After extracting the monthly LST time series, further processes such as statistical analysis were performed using Visual Basic for Applications (VBA) programming in Excel (Fig. 2).

2.3 Normalized difference Vegetation index (NDVI) extraction

Based on previous studies, variations in land use and land cover (LULC) patterns, vegetation density, and types can influence the synergistic operation and lapse rates of LST, especially across different elevation gradients. To assess the impact of these factors, we calculated the Normalized Difference Vegetation Index (NDVI) as a proxy for LULC classes, vegetation density, and types as suggested by (Cui et al. 2020). For this purpose, we used the Landsat 7 reflectance product during the growing season (April-September) to prepare an annual mean NDVI time series. All images with cloud cover less than 30% were utilized, and bit masks were applied to mask cloud shadows and snow. Finally, we implemented a gap-filling algorithm (Yan & Roy 2018) to obtain reflectance data for pixels affected by clouds, cloud shadows, or Scan Line Corrector (SLC) failures.

2.4 Trend detection based on linear regression

Linear least squares (SL) regression is a common method for detecting linear trends in climate time series, as demonstrated by Eklundh and Jönsson (2016). In this method, the observed climate variable and the time sequences are respectively considered as the response variable Y and the independent variable X (as shown in Eq. (1)). The slope and intercept coefficients (β0 and β1) in the best-fitting line can be determined using the Least Squares (LS) technique. This method aims to find coefficient values that minimize the squared differences between the observed and predicted values of Y.

(Huang et al. 2022).

$$Y = \beta_0 + \beta_1 X \tag{1}$$

The trend derived from SL is determined by the slope coefficient, and its LS estimate, which can be expressed as Eq. 2:

$$\beta_1 = \frac{\sum (x - \bar{x}) \times (y - \bar{y})}{\sum (x - \bar{x})^2} \tag{2}$$

The sign of the slope coefficient thus indicates trend direction (i.e., positive upward and negative downward). Significance of upward/downward trends is determined by the p-value of the slope coefficient (Huang et al. 2022).

3 Results

3.1 Spatial–temporal variability and change (2001–2021) of LSTs across the central alborz

3.1.1 Correlation analysis of land surface temperature changes in eastern region

The correlation heatmap for changes in LST across the Eastern study region is presented in Fig. 3. Based on the results, LST increases were observed in both mid-summer (June–July) and mid-winter (December–January) on the northern aspect at various elevations. Some of these increases showed statistical significance, such as r = 0.38 in January at 3500 m a.s.l. However, significant temperature decreases were only noted in October, with a correlation of − 0.54 at 2500 m a.s.l. Similar temperature patterns were found on the southern aspect, with the exception of June. Notably, significant temperature increases were recorded in July (r = 0.72 at 1500 m a.s.l.), January (r = 0.51 at 4000 m a.s.l.), and December (r = 0.42 at 2000 m a.s.l).

	(m)	Jan	Feb	Mar	Apr	May	Jun	Jul	Aug	Sep	Oct	Nov	Dec
Northern aspect	1500	0.35	-0.07	-0.27	-0.14	0.38	0.43	0.46	-0.06	-0.22	-0.44	-0.27	0.23
	2000	0.33	-0.01	-0.08	-0.02	0.18	0.33	0.55	-0.14	-0.14	-0.52	-0.24	0.25
	2500	0.26	0.08	-0.08	-0.12	-0.12	0.22	0.48	-0.21	0.03	-0.54	-0.14	0.29
	3000	0.32	0.13	-0.04	-0.11	-0.15	0.19	0.44	-0.15	0.11	-0.44	-0.05	0.33
	3500	0.38	0.1	-0.05	-0.09	-0.19	0.16	0.26	-0.22	0.03	-0.37	-0.07	0.33
	4000	0.28	0.09	-0.06	-0.05	-0.14	0.13	0.17	-0.25	-0.04	-0.39	-0.08	0.27
Southern aspect	1500	0.13	-0.11	-0.21	-0.18	-0.23	-0.15	0.72	-0.1	-0.21	-0.35	-0.35	0.34
	2000	0.26	-0.08	-0.26	-0.23	-0.24	-0.16	0.6	-0.27	-0.22	-0.39	-0.35	0.42
	2500	0.39	0.1	-0.25	-0.27	-0.25	-0.16	0.51	-0.27	-0.22	-0.4	-0.32	0.36
	3000	0.44	0.22	-0.23	-0.3	-0.28	-0.17	0.43	-0.23	-0.21	-0.38	-0.26	0.34
	3500	0.47	0.32	-0.14	-0.27	-0.32	-0.2	0.25	-0.27	-0.21	-0.35	-0.13	0.29
	4000	0.51	0.27	-0.16	-0.26	-0.34	-0.23	0.2	-0.37	-0.21	-0.38	-0.17	0.24

Fig. 2 R coefficient values calculated for changes in LSTs on northern and southern aspects, Eastern study region, Central Alborz (* = significance level of 0.05%; ** = significance level of 0.02%)

	(m)	Jan	Feb	Mar	Apr	May	Jun	Jul	Aug	Sep	Oct	Nov	Dec
Northern aspect	**1500**	5.68	8.7	15.21	19.46	22.3	24.45	25.17	25.34	22.8	17.97	11.42	7.18
	2000	2	4.99	12.66	19.43	22.86	26.17	26.88	26.95	23.78	17.71	9.47	3.87
	2500	-1.38	1.72	10.93	20.46	25.97	31.46	33.27	32.69	27.96	19.13	8.4	0.84
	3000	-4.65	-1.99	6.63	17.47	24.22	30.81	33.3	32.7	27.39	17.49	5.74	-2.56
	3500	-8.01	-5.53	1.58	11.54	19.76	27.64	30.45	29.69	24.06	13.74	1.79	-6.12
	4000	-10.18	-7.58	-1.42	7.72	16.36	25.02	28.02	27.09	21.31	11.08	-0.96	-8.3
Southern aspect	**1500**	10.34	16.56	23.99	31.8	39.15	43.54	46.47	45.7	38.61	29.57	19.55	11.57
	2000	6.77	11.87	19.71	26.48	33.15	38.53	41.88	40.98	34.17	25.49	15.84	8.32
	2500	1.55	5.41	14.03	21.4	27.72	33.9	37.61	36.74	30.05	21.17	11.21	3.45
	3000	-2.48	0.43	8.79	16.55	22.8	29.53	33.57	32.91	26.38	17.49	7.46	-0.61
	3500	-6.77	-4.31	2.59	10.56	18.29	25.73	29.9	29.45	22.95	13.81	2.79	-5.35
	4000	-8.37	-6.18	0.08	6.59	14.6	23.75	27.82	27.05	20.28	11.02	0.35	-7.26

Fig. 3 Average monthly LSTs (°C) for different elevation zones on northern and southern aspects of the Central Alborz in Between 2001 and 2021 (Eastern study region)

3.1.2 Altitudinal temperature trends and seasonal changes

On the northern aspect, maximum LSTs are reached during August at elevations of 1500 m a.s.l. (25.34 °C) and 2000 m a.s.l. (26.95 °C) (Fig. 3). At higher elevations, maximum LSTs are reached during July, suggesting an earlier onset of seasonal cooling here (i.e., from August onwards). During winter (December–March), LSTs turn negative, reaching coldest conditions in January at 4000 m a.s.l. (– 10.18 °C). In March, negative mean LSTs are only measured at 4000 m a.s.l. Very notable is the increase in mean temperature at 2500 m a.s.l. (17.62 °C) compared to that at 2000 m a.s.l. (16.40 °C) (Fig. 4). This reflects a strong temperature inversion, which may be a consequence of land use (i.e., land cover and hence surface albedo). Land use classes are more diverse (i.e., including gardens, forests with variable canopy cover, pastures with good cover and others with poor cover, rainfed and irrigated lands etc.) for the 2500 m a.s.l. class than 2000 m a.s.l. class, while forests with dense canopy cover a larger area at the 2000 m a.s.l. class than 2500 m a.s.l. class. LSTs are notably higher on the southern aspect. Mean annual LSTs, considering all elevations in this study, are 14.57 °C for the northern aspect and 18.70 °C for the southern aspect (Fig. 4). All elevations on the southern aspect have their highest mean LSTs in July, ranging from 46.47 °C at 1500 m a.s.l. to 27.82 °C at 4000 m a.s.l. Negative LSTs during winter months (December to February) are more confined to higher elevations and exhibit a lower amplitude of freezing on the northern aspect. (see Fig. 3).

3.1.3 Decadal trends in land surface temperatures (LST) from 2001 to 2021 across different elevations and aspects

The results of this section focus on decadal rates of change in LSTs within elevation zones ranging from 1500 to 4000 m above sea level, covering the period from 2001 to

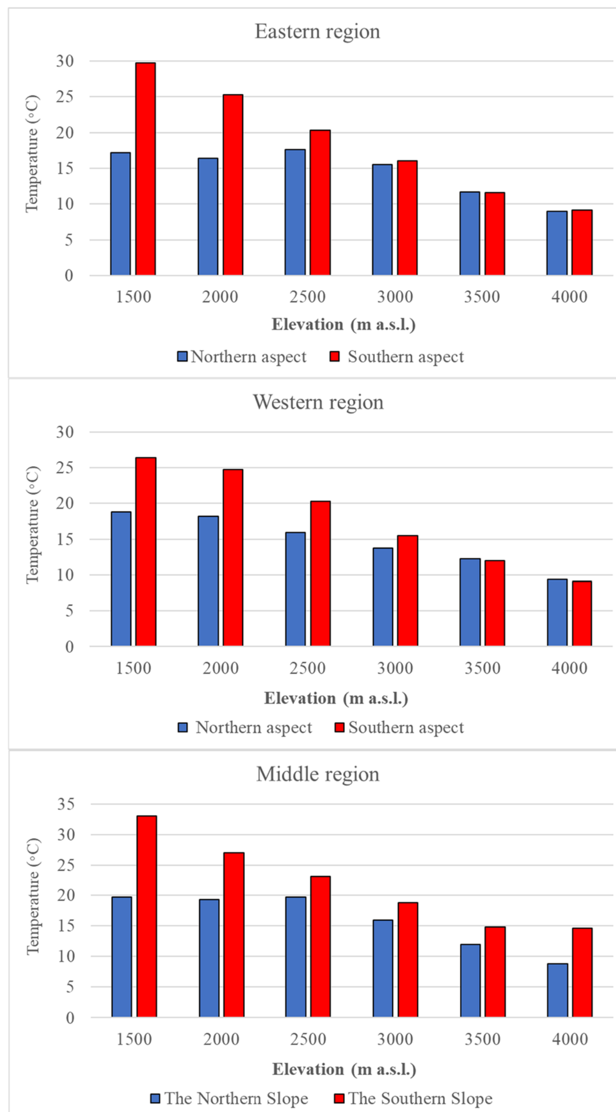

Fig. 4 Mean LSTs for different elevation zones (northern and southern aspects) of the three study regions, Central Alborz

	(m)	Jan	Feb	Mar	Apr	May	Jun	Jul	Aug	Sep	Oct	Nov	Dec
Northern aspect	1500	2.12	-1.17	-2.09	0.33	0.76	1.01	1.19	-0.23	-0.44	-1.57	-1.23	0.94
	2000	2.2	-0.84	-1.77	0.45	0.36	0.84	1.51	-0.4	-0.34	-1.99	-1.31	1.34
	2500	2.01	-0.1	-2.01	0.17	-0.41	0.61	1.24	-0.46	0.2	-2.19	-1.15	1.84
	3000	2.15	0.22	-1.61	0.34	-0.69	0.58	1.13	-0.25	0.52	-1.95	-0.93	1.98
	3500	2.15	0.17	-1.33	0.4	-0.98	0.47	0.7	-0.34	0.34	-1.81	-0.97	1.86
	4000	1.31	-0.01	-1.09	0.59	-0.76	0.39	0.5	-0.4	0.19	-2.02	-1.25	1.2
Southern aspect	1500	0.87	-0.8	-2.4	-1.74	-3.85	-3.11	2.08	0.01	-3.23	-4.37	-1.99	0.97
	2000	1.98	-0.61	-2.93	-2.06	-3.6	-3.07	1.46	-0.19	-2.95	-4.37	-1.86	1.59
	2500	3.07	0.24	-2.88	-1.96	-3.25	-2.65	1.3	-0.3	-2.55	-4.05	-1.92	2.06
	3000	3.3	0.99	-2.52	-1.5	-3.14	-2.38	1.07	-0.39	-2.18	-3.43	-1.76	2.26
	3500	3.21	1.39	-1.53	-0.83	-3.08	-2.38	0.7	-0.59	-1.96	-2.83	-1.68	1.64
	4000	3.74	1.08	-1.47	-0.86	-2.71	-2.56	0.57	-0.84	-1.87	-2.7	-1.94	1.61

Fig. 5 Average decadal changes of monthly LSTs (°C/decade) for different elevation zones on northern and southern aspects of the Central Alborz (Eastern study region)

2021 (see Fig. 5). For all elevations, LSTs increase during the January (+ 2 °C/decade), April (+ 0.4 °C/decade), June (+ 0.7 °C/decade), July (+ 1 °C/decade) and December (+ 1.5 °C/decade). In contrast, LSTs have decreased during the February (– 0.3 °C/decade), March (– 1.7 °C/decade), August (– 0.3 °C/decade), October (– 1.9 °C/decade), and November (– 1.1 °C/decade) (Fig. 6). In May and September, LST trends are unidirectional, depending on elevation. For example, this month, LSTs increase by + 0.6 °C/decade for both 1500 and 2000 m a.s.l. elevation zones, while they decrease by – 0.7 °C/decade for elevation zones 2500 to 4000 m a.s.l. Our results indicated + 0.003 °C/decade mean annual LST change for all elevations between the years 2001 and 2021 on the northern aspect (Fig. 4). Here, mean LST has decreased by – 0.11 °C/decade at 4000 m a.s.l., but has increased by 0.12 °C/decade at 3000 m a.s.l. (Fig. 7). At 2000 m a.s.l. the increase has been more marginal (+ 0.004 °C/decade). Results show that for the southern aspect, four months record positive LST changes (mean for all elevations): January (+ 2.70 °C/decade), February (+ 0.38 °C/decade), July (+ 1.20 °C/decade) and December (+ 1.69 °C/decade). Other months record negative LST changes, with the strongest mean cooling trend in October (– 3.63 °C/decade). The overall mean LST change for all months and elevations on the southern aspect is – 1.01 °C/decade (Fig. 4; Fig. 9). Decreasing LSTs here range from -1.46 °C/decade at 1500 m a.s.l. to -0.66 °C/decade at elevation zones 3500 and 4000 m a.s.l.

The monthly characteristics of lapse rates, considering each elevation class, are presented in Fig. 10. As can be observed, for the N aspect, strongest lapse rates (– 0.72 °C/100 m) are for elevation classes 3000 to 3500 m a.s.l., while for the S aspect strongest lapse rates (– 0.98 °C/100 m) are for elevation classes 2000– 2500 m a.s.l.

For the northern aspect, positive average lapse rates (indicating temperature inversions) are observed in the months of June (+ 0.02 °C/100 m), July (+ 0.11 °C/100 m), and August (+ 0.07 °C/100 m). The strongest negative lapse rate (–0.66 °C/100 m) is recorded in March (as shown in Fig. 8 and Fig. 9). In contrast, the southern aspect exhibits much stronger lapse rates, ranging from – 1.01 °C/100 m in April to – 0.71 °C/100 m in August (as indicated in Fig. 8 and Fig. 9). Overall mean annual lapse rates for all elevations are – 0.28 °C/100 m for the N aspect and – 0.82 °C/100 m for the S aspect, thus indicating large differences in cooling according to slope aspect (Fig. 10).

3.2 The western region of central Alborz

The results of the LST trend analysis in the Western region of Central Alborz are presented in Fig. 11 Based on the results, LSTs have increased at all elevations on the northern aspect of the western study region, during the months of January, May, June, July, and December (Fig. 11). Some such increases are significant at the 0.05 percentage level. In summary, notable positive correlations were observed in various months, including January (r = 0.42 at 2000 m and 3000 m a.s.l.), May (r = 0.41 at 1500 m a.s.l.), June (r = 0.59 at 1500 m a.s.l.), July (r = 0.55 at 1500 m a.s.l.), and December (r = 0.53 at 4000 m a.s.l). However, LSTs exhibited significant decreases (at a 0.05% significance level) in October for different elevation zones, with the strongest decreasing trend (r = -0.52) observed at 1500 m a.s.l (more information in Fig. 11).

3.2.1 Seasonal and elevation-dependent patterns of land surface temperatures (LSTs) on northern and southern aspects of the central Alborz

On the northern aspect, maximum LSTs are reached during August at elevations of 3500 m a.s.l. (31.41 °C) and 3000 m a.s.l. (30.57 °C) (Fig. 12). At higher elevations, maximum LSTs occur in July, indicating an earlier onset of

Fig. 6 Comparison of LST changes (°C/decade) for different elevation zones (northern and southern aspects) of the three study regions, Central Alborz

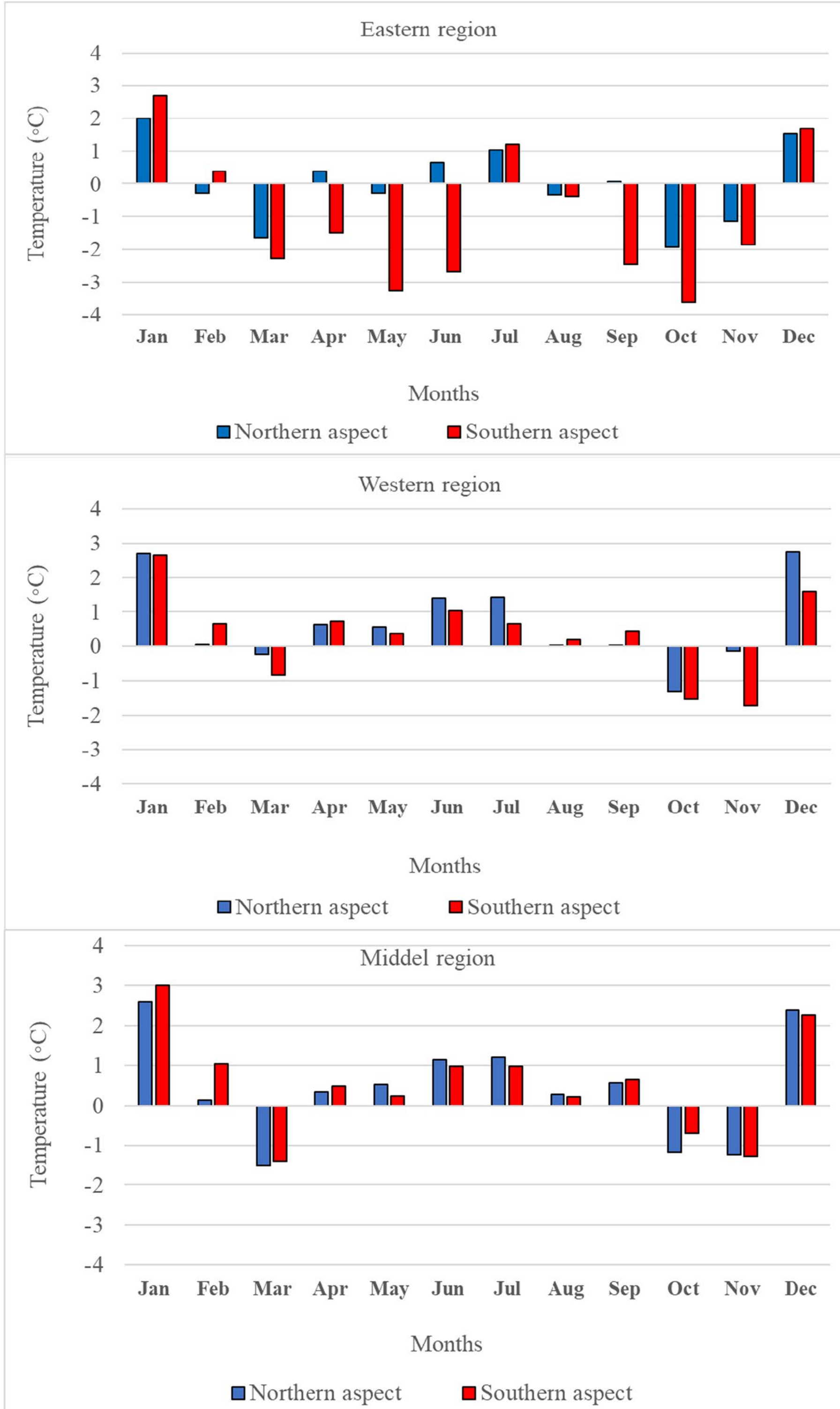

cooling, usually beginning in August. Sub-zero temperatures are recorded as follows: November at 4000 m a.s.l.; December at 3000–4000 m a.s.l.; January at 2000–4000 m a.s.l. (coldest at 4000 m a.s.l., – 9.78 °C); February at 3000–4000 m a.s.l.; and March at 4000 m a.s.l. (Fig. 12).

As expected, LSTs are considerably higher on the southern aspect. Mean annual LSTs across all elevations considered in this study are 14.70 °C for the northern aspect and 18.01 °C for the southern aspect (Fig. 4). In August, the southern aspect records its highest mean LSTs, varying from

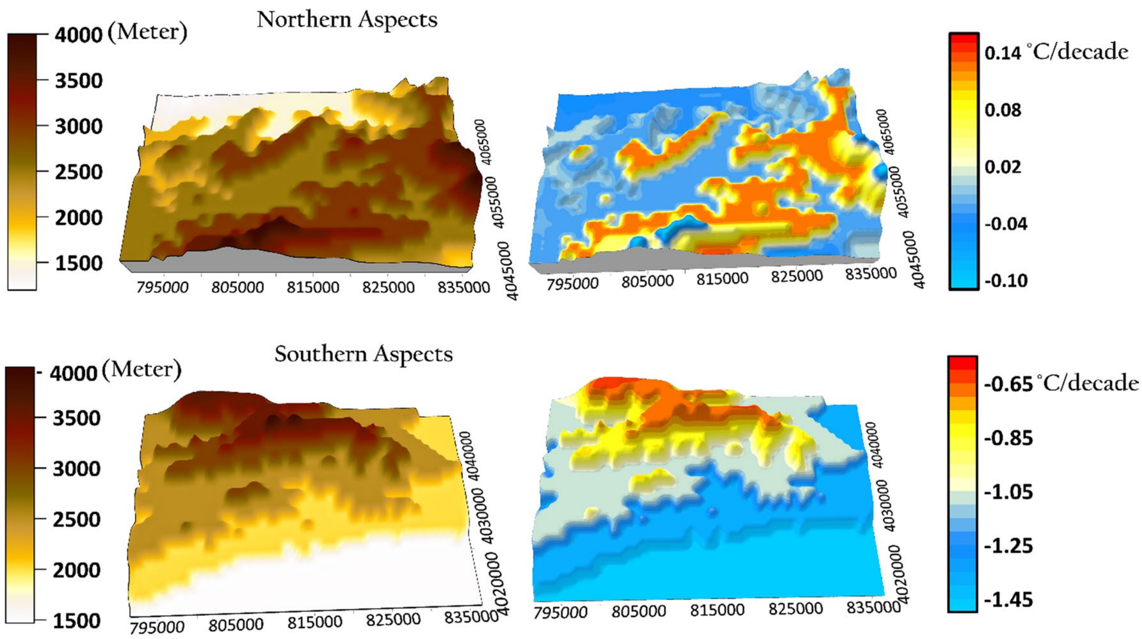

Fig. 7 Spatial distribution of LST changes (°C/decade) for northern and southern aspects of the Central Alborz (Eastern study region)

	(m)	Jan	Feb	Mar	Apr	May	Jun	Jul	Aug	Sep	Oct	Nov	Dec
The N slope	2000-1500	-0.74	0.04	-0.51	0	0.11	0.34	0.34	0.32	0.2	-0.05	-0.39	-0.66
	2500-2000	-0.68	-0.65	-0.34	0.2	0.62	1.06	1.28	1.15	0.84	0.28	-0.22	-0.61
	3000-2500	-0.65	0.04	-0.86	-0.6	-0.35	-0.13	0.01	0	-0.11	-0.33	-0.53	-0.68
	3500-3000	-0.67	-0.04	-1.01	-1.19	-0.89	-0.64	-0.57	-0.6	-0.67	-0.75	-0.79	-0.71
	4000-3500	-0.43	-0.02	-0.6	-0.76	-0.68	-0.52	-0.49	-0.52	-0.55	-0.53	-0.55	-0.44
The S slope	2000-1500	-0.71	-0.94	-0.86	-1.06	-1.2	-1	-0.92	-0.9	-0.89	-0.81	-0.74	-0.65
	2500-2000	-1.04	-1.29	-1.14	-1.02	-1.08	-0.92	-0.85	-0.81	-0.82	-0.86	-0.93	-0.97
	3000-2500	-0.81	-1	-1.05	-0.97	-0.99	-0.87	-0.81	-0.73	-0.73	-0.74	-0.75	-0.81
	3500-3000	-0.86	-0.95	-1.24	-1.2	-0.9	-0.76	-0.73	-0.66	-0.69	-0.73	-0.93	-0.95
	4000-3500	-0.32	-0.38	-0.5	-0.79	-0.74	-0.4	-0.42	-0.46	-0.54	-0.56	-0.49	-0.38

Fig. 8 Average monthly LST lapse rates (°C/100 m) for different elevation zones on northern and southern aspects of the Central Alborz (Eastern study region) over time

40.34 °C at 1500 m a.s.l. to 29.61 °C at 4000 m a.s.l. However, during winter (December–February), negative LSTs are confined to higher elevations and exhibit a lesser freeze amplitude compared to the northern aspect.

3.2.2 Decadal trends in land surface temperatures (LST) for elevation zones (1500-4000 m a.s.l.)—2001–2021

The decadal rates of change in LSTs for elevation zones ranging from 1500 to 4000 m a.s.l. during the period 2001–2021 are displayed in Fig. 13.For all elevations, LSTs increased during the January (+ 2.7 °C/decade), February (+ 0.1 °C/decade), April (+ 0.6 °C/decade), May (+ 0.6 °C/decade), June (+ 1.4 °C/decade), July (+ 1.4 °C/decade), August (+ 0.02 °C/decade), September (0.003 °C/decade), and December (+ 2.8 °C/decade). Negative decadal temperature changes are measured in the March (− 0.23 °C/decade), October (− 1.31 °C/decade) and November (− 0.13 °C/decade). Our results indicated a + 0.66 °C/decade mean annual LST change for all elevations between the years 2001 and 2021 on the northern aspect (Fig. 4). Within this region, mean LST increases vary from + 0.56 °C/decade at 1500 m a.s.l. to + 0.75 °C/decade at 4000 m a.s.l. (Fig. 6 and Fig. 13).

Results show that for the southern aspect, three months record LST cooling rates (mean for all elevations): March (− 0.85 °C/decade), October (− 1.53 °C/decade), and November (− 1.73 °C/decade). Other months record positive LST changes, with the strongest increase in January (+ 2.65 °C/decade). The overall mean LST change for all months and elevations on the southern aspect is + 0.35 °C/decade (Fig. 6 and Fig. 13). Decreasing LST (− 0.52 °C/

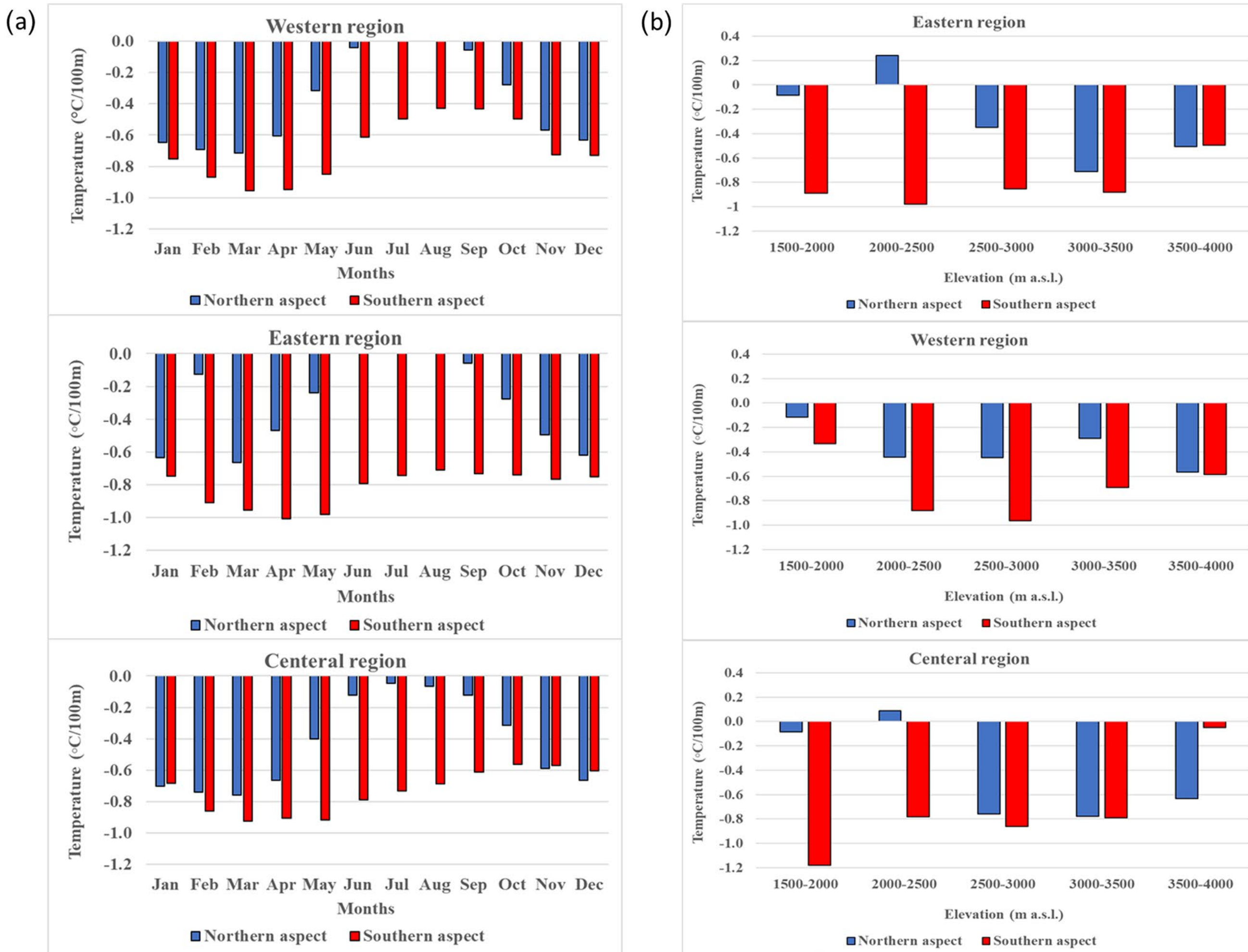

Fig. 9 **a** Monthly LST **b** Annual LST lapse rates (°C/100 m) for N- and S-facing slopes of the three Central Alborz regions (different altitude levels Between 2000–2021)

decade) is only recorded for the 1500 m a.s.l. class. Temperatures are increasing for all other elevation classes, with a maximum of + 0.66 °C/decade for the 2000 m a.s.l. class (Fig. 14). We thus note accelerated warming with increasing elevation (Fig. 10).

3.2.3 Lapse rates in the western study region: northern and southern aspects

For the N aspect, two months (July & August) record positive mean lapse rates or temperature inversions (+ 0.03 °C/100 m & + 0.04 °C/100 m respectively). The strongest negative lapse rate (– 0.71 °C/100 m) is recorded for March (Fig. 15 and Fig. 9). In contrast, all months record negative lapse rates on the S aspect, ranging from -0.96 °C/100 m in March to – 0.43 °C/100 m in August (Fig. 15 and Fig. 9). Mean annual lapse rates are – 0.37 °C/100 m for the N aspect and – 0.69 °C/100 m for the S aspect. Regarding the N aspect, the most pronounced lapse rate (– 0.56 °C/100 m) is observed within the elevation range of 3500 m a.s.l. to 4000 m a.s.l. Conversely, for the S aspect, the steepest lapse rate (– 0.96 °C/100 m) is evident between 2500 m a.s.l. and 3000 m a.s.l. (Fig. 16).

3.3 The Middle region of Central Alborz

3.3.1 Land surface temperature patterns in northern and southern aspects at various elevations

We note that LSTs have increased at all elevations for the northern aspect during the months of January, June, July and December (Fig. 17). Some such increases are significant at the 0.05 percentage level. For example, in January, June, July and December. Although LSTs are decreasing during other months, such decreases are only significant (at 0.05% significance level) in October for a variety of elevation zones

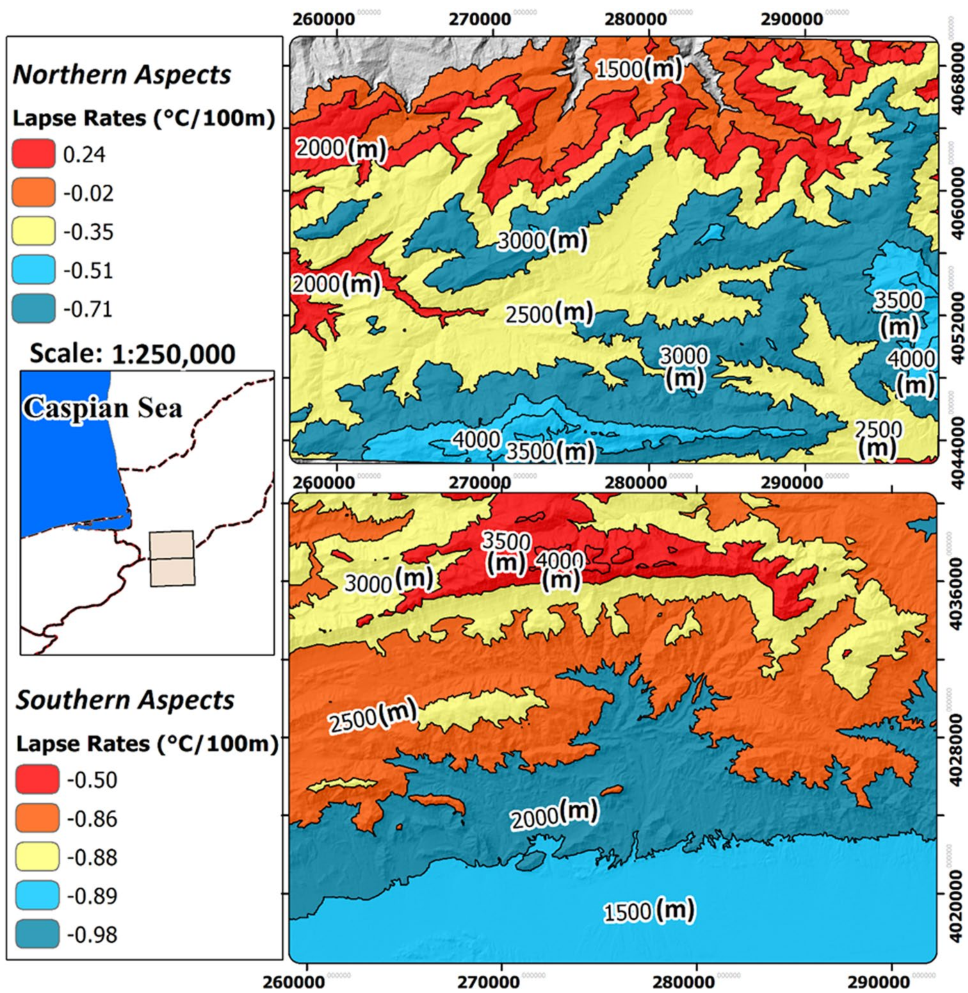

Fig. 10 Spatial distribution of mean annual LST lapse rates (°C/100 m) for northern and southern aspects of the Central Alborz (Eastern study region)

	(m)	Jan	Feb	Mar	Apr	May	Jun	Jul	Aug	Sep	Oct	Nov	Dec
The N slope	1500	0.41*	-0.11	0.05	-0.1	0.41*	0.59**	0.55**	-0.03	-0.03	-0.52**	-0.15	0.41*
	2000	0.42*	-0.07	0.09	0.02	0.34	0.53**	0.54**	-0.07	-0.01	-0.48**	-0.07	0.41*
	2500	0.41*	-0.01	0.1	0	0.23	0.36	0.47**	-0.13	0.01	-0.48**	-0.06	0.42*
	3000	0.42*	0.08	0.08	0.01	0.12	0.21	0.32	-0.14	0.06	-0.46*	-0.05	0.43*
	3500	0.38	0.08	0	0.02	0.11	0.12	0.21	-0.14	0.06	-0.41*	-0.03	0.47**
	4000	0.34	0.17	0.06	0.01	0.11	0.21	0.19	-0.15	0.06	-0.26	-0.04	0.53**
The S slope	1500	0.21	-0.17	-0.24	-0.07	-0.08	-0.07	0.07	-0.76	-0.27	-0.68**	-0.45*	0.15
	2000	0.42*	0.15	-0.11	0.03	0.07	0.37	0.53**	-0.18	0.11	-0.42**	-0.17	0.37
	2500	0.47**	0.21	0	0.03	0.12	0.35	0.50**	0.1	0.24	-0.28	-0.16	0.41*
	3000	0.46*	0.23	0.02	0	0.13	0.28	0.41*	0.14	0.26	-0.18	-0.1	0.33
	3500	0.46*	0.29	0.02	0.03	0.17	0.26	0.27	0.12	0.24	-0.2	-0.02	0.36
	4000	0.43*	0.26	0	0.02	0.07	0.23	0.21	0.06	0.18	-0.25	0.01	0.41*

Fig. 11 R coefficient values calculated for changes in LSTs on northern and southern aspects, Western study area, Central Alborz (* = significance level of 0.05%; ** = significance level of 0.02%)

(Fig. 17). Results for the southern aspect are not dissimilar, except for February, March, April, September and November, which record an increasing trend. Significant Land surface temperature increases (the maximum value of r) are measured for February at 4000 m a.s.l. (r = 0.85), March and April at 4000 m a.s.l. (r = 0.81), September at 4000 m a.s.l. (r = 0.55) and November at 4000 m a.s.l. (r = 0.82). (Fig. 17). Although LSTs are decreasing during other months, such decreases are only significant (at 0.05% significance level) in October at 1500 m a.s.l. (r = – 0.49). (Fig. 17).

	(m)	Jan	Feb	Mar	Apr	May	Jun	Jul	Aug	Sep	Oct	Nov	Dec
The N slope	**1500**	6.43	10.07	16.04	21.22	23.97	26.68	27.63	27.85	25.42	19.82	12.18	7.75
	2000	3.74	7.79	14.72	21.59	24.32	27.45	28.12	28.66	26.07	19.65	10.65	5.28
	2500	-0.2	3.3	10.5	19.58	23.26	27.16	27.82	28.37	25.35	17.69	7.2	1.29
	3000	-5.59	-2.55	4.52	15.85	22.7	28.49	30	30.57	26.08	15.75	2.54	-4
	3500	-7.92	-5.21	1.15	11.76	20.77	28.54	30.88	31.41	26.34	14.93	0.49	-6.2
	4000	-9.78	-7.28	-1.86	6.1	16.08	25.64	28.33	28.91	24.01	12.86	-2.01	-8.02
The S slope	**1500**	8.28	13.89	21.49	27.89	34.65	40.66	41.44	40.34	35.65	26.46	16.12	10.03
	2000	4.91	10.74	19.37	25.12	32.03	39.45	40.83	40.2	35.74	26.05	14.79	7.51
	2500	-0.96	3.37	13.07	20.88	27.63	35.71	37.77	37.61	33.02	22.92	10.6	2.13
	3000	-6.69	-3.3	4.48	14.51	23.1	32.02	34.81	35.14	30.28	19.88	5.41	-3.78
	3500	-8.79	-5.9	0.25	8.36	18.28	28.8	31.71	32.17	27.34	16.94	1.45	-6.26
	4000	-10.57	-7.84	-2.42	4.2	13.4	25.29	29.02	29.61	24.8	14.1	-2.04	-8.25

Fig. 12 Average monthly LSTs (°C) for different elevation zones on northern and southern aspects of the Central Alborz (Western study region)

	(m)	Jan	Feb	Mar	Apr	May	Jun	Jul	Aug	Sep	Oct	Nov	Dec
The N slope	**1500**	3.01	-0.68	-0.57	0.05	0.78	1.68	1.56	0.37	-0.2	-1.27	-0.32	2.26
	2000	3.42	-0.47	-0.41	0.39	0.64	1.78	1.81	0.29	-0.18	-1.4	-0.06	2.69
	2500	3.03	-0.12	-0.24	0.38	0.44	1.49	1.97	-0.03	-0.1	-1.53	-0.05	2.81
	3000	2.56	0.35	-0.04	0.75	0.25	1.22	1.46	-0.25	0.19	-1.43	-0.24	2.81
	3500	2.27	0.44	-0.31	1.17	0.46	0.9	0.92	-0.21	0.08	-1.21	-0.14	3.01
	4000	1.83	0.8	0.19	1.14	0.81	1.32	0.84	-0.04	0.23	-1.04	0.03	2.94
The S slope	**1500**	1.76	-0.66	-1.32	0.14	-0.24	-0.39	-0.02	-1.17	-0.56	-2.08	-1.85	0.14
	2000	3.68	0.54	-1.2	0.69	0.37	1.11	1.05	-0.04	0.32	-1.57	-1.57	1.77
	2500	3.75	1.32	-0.83	0.94	0.41	1.44	1.16	0.36	0.69	-1.4	-2.25	2.29
	3000	2.69	1.1	-0.68	0.8	0.43	1.33	0.92	0.54	0.77	-1.1	-2.35	1.63
	3500	2.19	0.99	-0.5	1.02	0.75	1.33	0.53	0.68	0.78	-1.29	-1.44	1.73
	4000	1.82	0.71	-0.53	0.8	0.57	1.36	0.26	0.73	0.65	-1.76	-0.9	1.98

Fig. 13 Average decadal changes of monthly LSTs (°C/decade) for different elevation zones on northern and southern aspects of the Central Alborz (Western study region)

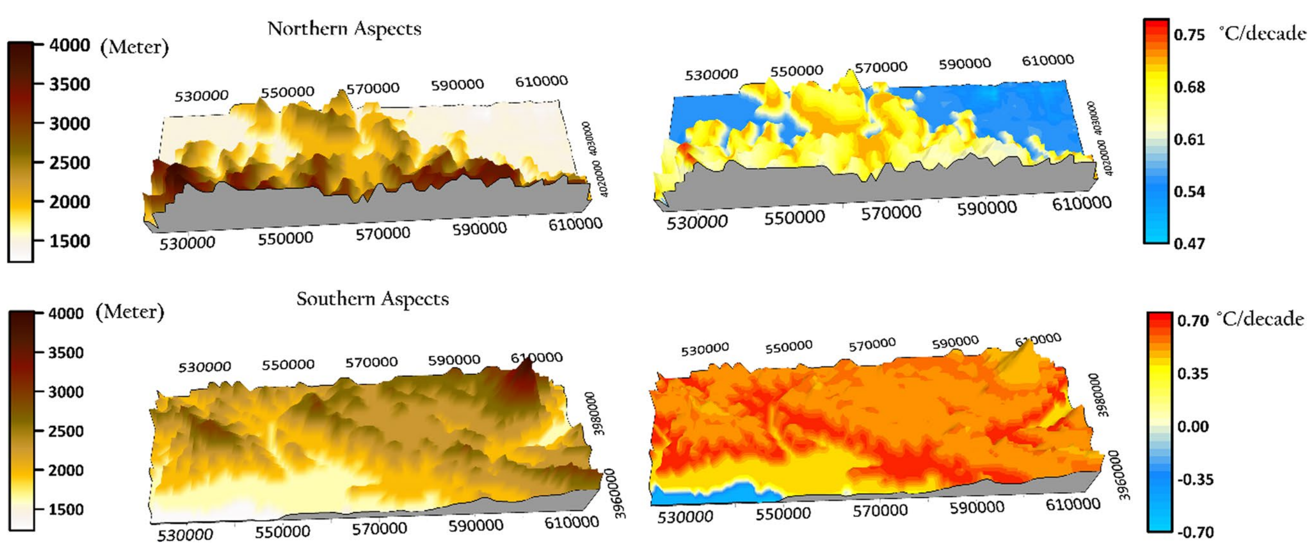

Fig. 14 Spatial distribution of LST changes (°C/decade) for northern and southern aspects of the Central Alborz (Western study region)

	(m)	Jan	Feb	Mar	Apr	May	Jun	Jul	Aug	Sep	Oct	Nov	Dec
The N slope	2000-1500	-0.54	-0.46	-0.26	0.07	0.07	0.15	0.1	0.16	0.13	-0.04	-0.31	-0.49
	2500-2000	-0.79	-0.9	-0.84	-0.4	-0.21	-0.06	-0.06	-0.06	-0.14	-0.39	-0.69	-0.8
	3000-2500	-1.08	-1.17	-1.2	-0.75	-0.11	0.27	0.44	0.44	0.15	-0.39	-0.93	-1.06
	3500-3000	-0.47	-0.53	-0.67	-0.82	-0.39	0.01	0.18	0.17	0.05	-0.16	-0.41	-0.44
	4000-3500	-0.37	-0.41	-0.6	-1.13	-0.94	-0.58	-0.51	-0.5	-0.47	-0.41	-0.5	-0.36
The S slope	2000-1500	-0.67	-0.63	-0.42	-0.55	-0.53	-0.24	-0.12	-0.03	0.02	-0.08	-0.27	-0.5
	2500-2000	-1.17	-1.47	-1.26	-0.85	-0.88	-0.75	-0.61	-0.52	-0.54	-0.63	-0.84	-1.08
	3000-2500	-1.15	-1.33	-1.72	-1.27	-0.9	-0.74	-0.59	-0.5	-0.55	-0.61	-1.04	-1.18
	3500-3000	-0.42	-0.52	-0.85	-1.23	-0.96	-0.64	-0.62	-0.59	-0.59	-0.59	-0.79	-0.49
	4000-3500	-0.36	-0.39	-0.53	-0.83	-0.98	-0.7	-0.54	-0.51	-0.51	-0.57	-0.7	-0.4

Fig. 15 Mean monthly LST lapse rates (°C/100 m) for different elevation zones on northern and southern aspects of the Central Alborz (Western study region) in over time

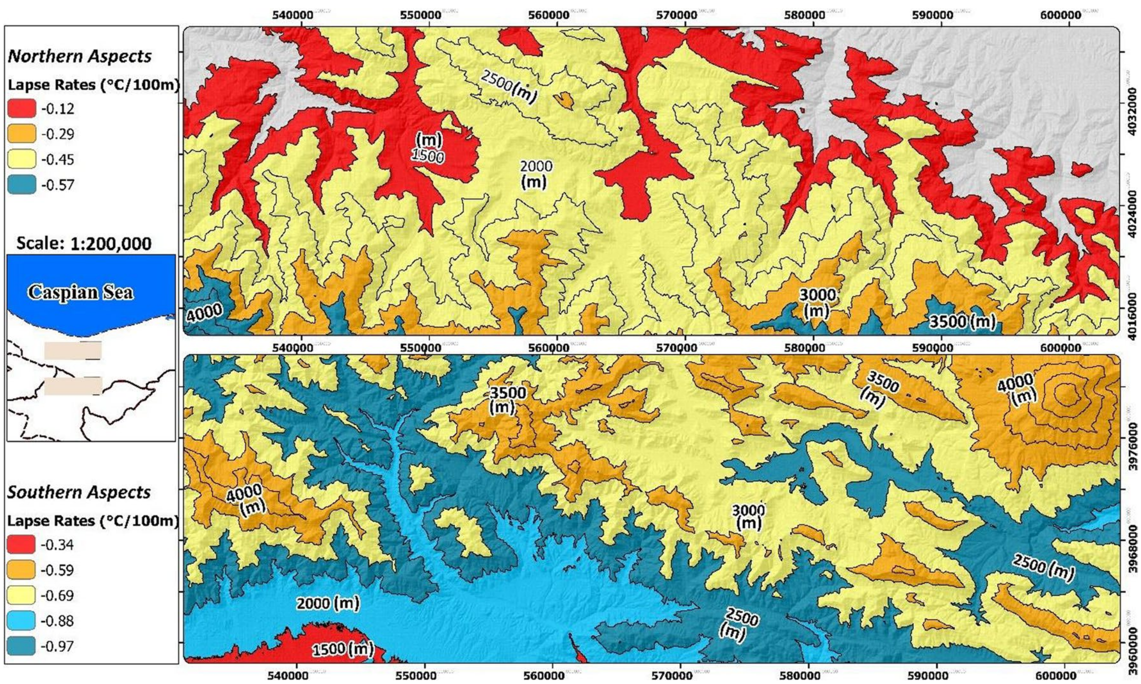

Fig. 16 Spatial distribution of mean annual LST lapse rates (°C/100 m) for northern and southern aspects of the Central Alborz (Western study region)

	(m)	Jan	Feb	Mar	Apr	May	Jun	Jul	Aug	Sep	Oct	Nov	Dec
The N slope	**1500**	0.36	-0.13	-0.13	-0.03	0.49**	0.63**	0.57**	0.04	0.1	-0.51**	-0.27	0.37
	2000	0.41*	-0.03	-0.06	0.06	0.28	0.50**	0.61**	0.02	0.13	-0.55**	-0.22	0.41*
	2500	0.48**	0.16	-0.05	-0.04	-0.03	0.25	0.55**	-0.05	0.17	-0.41*	-0.09	0.44*
	3000	0.43*	0.15	-0.06	-0.06	-0.04	0.19	0.41**	-0.05	0.22	-0.28	-0.02	0.41*
	3500	0.42*	0.17	-0.09	-0.07	0.27	0.21	0.24	-0.04	0.19	-0.15	0.02	0.36
	4000	0.41*	0.21	-0.07	-0.04	0.33	0.24	0.12	-0.06	0.16	-0.16	0.04	0.37
The S slope	**1500**	0.27	0.11	-0.07	0.09	0.06	0.47**	0.66**	-0.04	0.18	-0.49**	-0.28	0.41*
	2000	0.37	0.1	-0.11	-0.02	-0.07	0.37	0.61**	-0.01	0.17	-0.35	-0.17	0.43*
	2500	0.45*	0.18	-0.1	-0.05	-0.12	0.26	0.54**	0.09	0.22	-0.16	-0.12	0.47**
	3000	0.47**	0.24	-0.11	-0.06	-0.11	0.18	0.42*	0	0.18	-0.03	-0.05	0.44*
	3500	0.47**	0.27	-0.1	-0.09	-0.03	0.16	0.28	-0.09	0.15	-0.04	0.05	0.37
	4000	0.72**	0.85**	0.81**	0.81**	0.47**	0.61**	0.19	0.15	0.55**	0.50**	0.47**	0.82**

Fig. 17 R coefficient values calculated for changes in LSTs on northern and southern aspects, the Middle region study area, Central Alborz (* = significance level of 0.05%; ** = significance level of 0.02%)

On the northern aspect, the highest LSTs are attained in August at elevations of 2500 m a.s.l. (35.50 °C) (see Fig. 18). At higher elevations, the maximum LSTs occur in July, indicating an earlier initiation of seasonal cooling. (i.e., from August onwards). Negative Land surface temperature values are measured in January for elevation classes 2500–4000 m a.s.l. (coldest conditions at 4000 m a.s.l. = − 10.18 °C), in February for 3000 to 4000 m a.s.l. (coldest conditions at 4000 m a.s.l. = − 7.64 °C), in March and November for 4000 m a.s.l. (− 2.08 °C and − 1.38 °C respectively) and in December for 3000–4000 m a.s.l. (coldest conditions at 4000 m a.s.l. = − 8.09 °C) (Fig. 18).

As expected, LSTs are considerably higher on the southern aspect. Mean annual LSTs across all elevations considered in this study are 15.87 °C for the northern aspect and 21.90 °C for the southern aspect (Fig. 4). All elevations on the southern aspect have their highest mean LSTs in July, ranging from 49.56 °C at 1500 m a.s.l. to 31.50 °C at 4000 m a.s.l. Mean negative LSTs during winter months (December to February) are more elevationally constrained (i.e., to higher elevations) and have a lower amplitude of freeze than on the northern aspect (see Fig. 18 to compare).

The results of decadal rates of change in LSTs for the different elevation zones and for the study period is presented in Fig. 19. For all elevations, LSTs increase during the months of January (+ 2.60 °C/decade), February (+ 0.13 °C/decade), April (+ 0.34 °C/decade), May (+ 0.53 °C/decade), June (+ 1.15 °C/decade), July (+ 1.21 °C/decade), August (+ 0.28 °C/decade), September (+ 0.57 °C/decade) and December (+ 2.38 °C/decade). Mean decadal cooling is recorded for the months of March (–1.52 °C/decade), October (–1.18 °C/decade) and November (− 1.24 °C/decade).

Our results indicated an overall + 0.44 °C/decade mean annual LST change for all elevations over the years 2001–2021 on the northern aspect (Fig. 4). In a way that the mean LST has increased from a minimum of + 0.30 °C/decade at 1500 m a.s.l. to a maximum of + 0.70 °C/decade at 2500 m a.s.l. (Fig. 6 and Fig. 19).

Results show that for the southern aspect, three months record negative LST changes (mean for all elevations):

	(m)	Jan	Feb	Mar	Apr	May	Jun	Jul	Aug	Sep	Oct	Nov	Dec
The N slope	1500	7.36	10.84	16.93	22.07	25.09	27.95	28.51	28.87	25.79	20.63	13.36	8.52
	2000	4.03	7.89	15.17	22.01	25.65	29.75	30.16	30.83	27.23	20.69	11.74	5.65
	2500	-0.45	3.79	13.36	22.25	27.45	33.93	35.35	35.5	30.7	21.61	10.34	2.27
	3000	-4.57	-1.31	6.85	17.37	24.01	31.33	33.36	33.28	28.2	18.43	5.88	-2.26
	3500	-8.1	-5.34	1.11	10.62	19.73	28.23	30.52	30.37	25.56	15.57	1.6	-5.98
	4000	-10.18	-7.64	-2.08	5.46	15	24.88	27.34	27.2	22.72	12.77	-1.38	-8.09
The S slope	1500	12.93	19.1	27.26	34.68	42.71	48.55	49.56	48.72	43.52	33.6	22.04	13.89
	2000	6.33	12	21.08	28.15	35.88	42.88	44.23	43.3	38	27.88	16.21	8.35
	2500	1.38	5.98	16.01	24.13	31.53	39.61	41.37	40.62	35.11	24.6	12.58	4.33
	3000	-3.18	0.23	9.33	19.69	27.19	35.81	37.64	37.21	31.78	21.28	8.88	-0.25
	3500	-6.19	-3.55	3.35	12.72	22.16	31.95	34.09	33.97	29.07	18.87	5.3	-3.51
	4000	-4.17	-2.39	4.12	12.06	19.78	28.85	31.28	31.5	28.21	19.56	7.77	-1.27

Fig. 18 Average monthly LSTs (°C) for different elevation zones on northern and southern aspects of the Central Alborz (Middle study region)

	(m)	Jan	Feb	Mar	Apr	May	Jun	Jul	Aug	Sep	Oct	Nov	Dec
The N slope	1500	2.32	-1.31	-1.73	0.61	1.21	1.49	1.45	0.43	0.17	-1.41	-1.45	1.87
	2000	3.04	-0.69	-1.66	0.76	0.97	1.53	1.95	0.38	0.28	-1.87	-1.56	2.51
	2500	4.18	0.89	-1.61	0.31	0.28	1.17	1.85	0.29	0.59	-1.28	-1.28	3.04
	3000	2.64	0.72	-1.63	0.23	0.12	1.00	1.30	0.20	0.82	-1.07	-1.24	2.59
	3500	1.86	0.59	-1.47	0.02	0.24	0.87	0.66	0.19	0.81	-0.66	-1.06	2.17
	4000	1.54	0.58	-1.04	0.11	0.37	0.84	0.06	0.17	0.72	-0.79	-0.87	2.08
The S slope	1500	2.10	0.62	-0.71	1.02	0.59	0.89	1.39	0.21	0.68	-1.32	-1.51	1.65
	2000	3.34	0.55	-1.37	0.43	0.25	1.10	1.36	0.31	0.60	-1.12	-1.39	2.23
	2500	4.03	0.9	-1.69	0.3	-0.02	1.06	1.39	0.38	0.79	-0.77	-1.49	2.72
	3000	3.32	1.27	-1.77	0.36	-0.12	1.05	1.24	0.16	0.75	-0.49	-1.54	2.62
	3500	2.49	1.22	-1.54	0.28	0.12	0.91	0.59	0.06	0.61	-0.4	-1.08	2.14
	4000	2.80	1.64	-1.43	0.55	0.56	0.85	-0.08	0.17	0.43	-0.06	-0.76	2.24

Fig. 19 Average decadal changes of monthly LSTs (°C/decade) for different elevation zones on northern and southern aspects of the Central Alborz (Middle study region)

March (–1.42 °C/decade), October (–0.69 °C/decade), and November (–1.30 °C/decade). Other months record positive LST changes, with the strongest mean warming trend for January (+3.01 °C/decade). The mean annual LST change on the southern aspect is + 0.54 °C/decade (Fig. 19; Fig. 6). Increasing LST varies from + 0.45 °C/decade at 3500 m a.s.l. to + 0.63 °C/decade at 2500 m a.s.l. Thus, for the Middle region of the Central Alborz, strongest warming is recorded at lower elevations (Fig. 20).

Lapse rates on the northern aspect vary from –0.76 °C/100 m in March to – 0.05 °C/100 m in July, while those for the southern aspect range from -0.92 °C/100 m in May to – 0.56 °C/100 m in October (Fig. 21 and Fig. 9). Mean annual lapse rates are – 0.43 °C/100 m for the northern aspect and – 0.74 °C/100 m for the southern aspect. For the northern aspect, the strongest lapse rate (– 0.78 °C/100 m) occurs between elevation classes 3000 m a.s.l. and 3500 m a.s.l., while that for the southern aspect (– 1.20 °C/100 m) is between 1500 m a.s.l. and 2000 m a.s.l. (Fig. 22).

3.4 Effects of land use class and vegetation types on synergistic operation and LST lapse rates

The mean NDVI for the various elevation zones (northern and southern aspects) in the three study regions of the Central Alborz shows higher values for the northern aspect (0.291) compared to the southern aspect (0.101) (see Fig. 23). NDVI values also vary longitudinally across

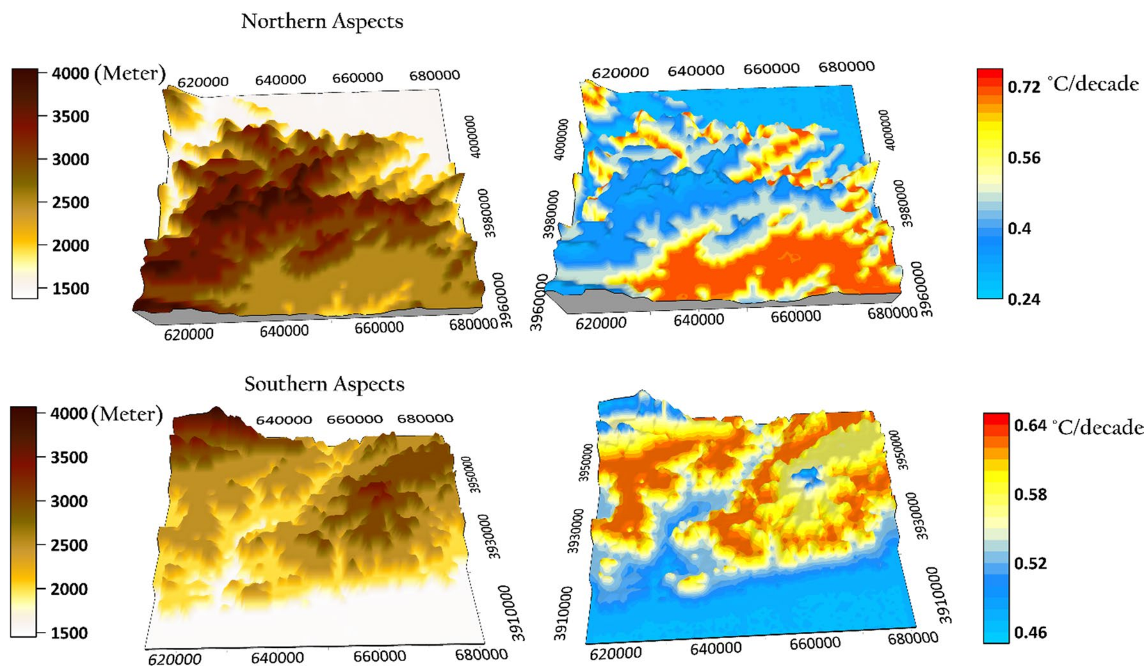

Fig. 20 Spatial distribution of LST changes (°C/decade) for northern and southern aspects of the Central Alborz (Middle study region)

	(m)	Jan	Feb	Mar	Apr	May	Jun	Jul	Aug	Sep	Oct	Nov	Dec
The N slope	2000-1500	-0.67	-0.59	-0.35	-0.01	0.11	0.36	0.33	0.39	0.29	0.01	-0.32	-0.57
	2500-2000	-0.9	-0.82	-0.36	0.05	0.36	0.84	1.04	0.93	0.69	0.18	-0.28	-0.68
	3000-2500	-0.82	-1.02	-1.3	-0.98	-0.69	-0.52	-0.4	-0.44	-0.5	-0.64	-0.89	-0.91
	3500-3000	-0.71	-0.81	-1.15	-1.35	-0.86	-0.62	-0.57	-0.58	-0.53	-0.57	-0.86	-0.75
	4000-3500	-0.42	-0.46	-0.64	-1.03	-0.94	-0.67	-0.64	-0.63	-0.57	-0.56	-0.6	-0.42
The S slope	2000-1500	-1.32	-1.42	-1.24	-1.31	-1.37	-1.13	-1.07	-1.08	-1.1	-1.14	-1.17	-1.11
	2500-2000	-0.99	-1.21	-1.01	-0.8	-0.87	-0.65	-0.57	-0.54	-0.58	-0.66	-0.73	-0.8
	3000-2500	-0.91	-1.15	-1.34	-0.89	-0.87	-0.76	-0.74	-0.68	-0.66	-0.66	-0.74	-0.91
	3500-3000	-0.6	-0.76	-1.19	-1.39	-1.01	-0.77	-0.71	-0.65	-0.54	-0.48	-0.72	-0.65
	4000-3500	0.4	0.23	0.15	-0.13	-0.47	-0.62	-0.56	-0.49	-0.17	0.14	0.49	0.45

Fig. 21 Mean monthly LST lapse rates (°C/100 m) for different elevation zones on northern and southern aspects of the Central Alborz (Middle study region) in over time

Fig. 22 Spatial distribution of mean annual LST lapse rates (°C/100 m) for northern and southern aspects of the Central Alborz (Middle study region)

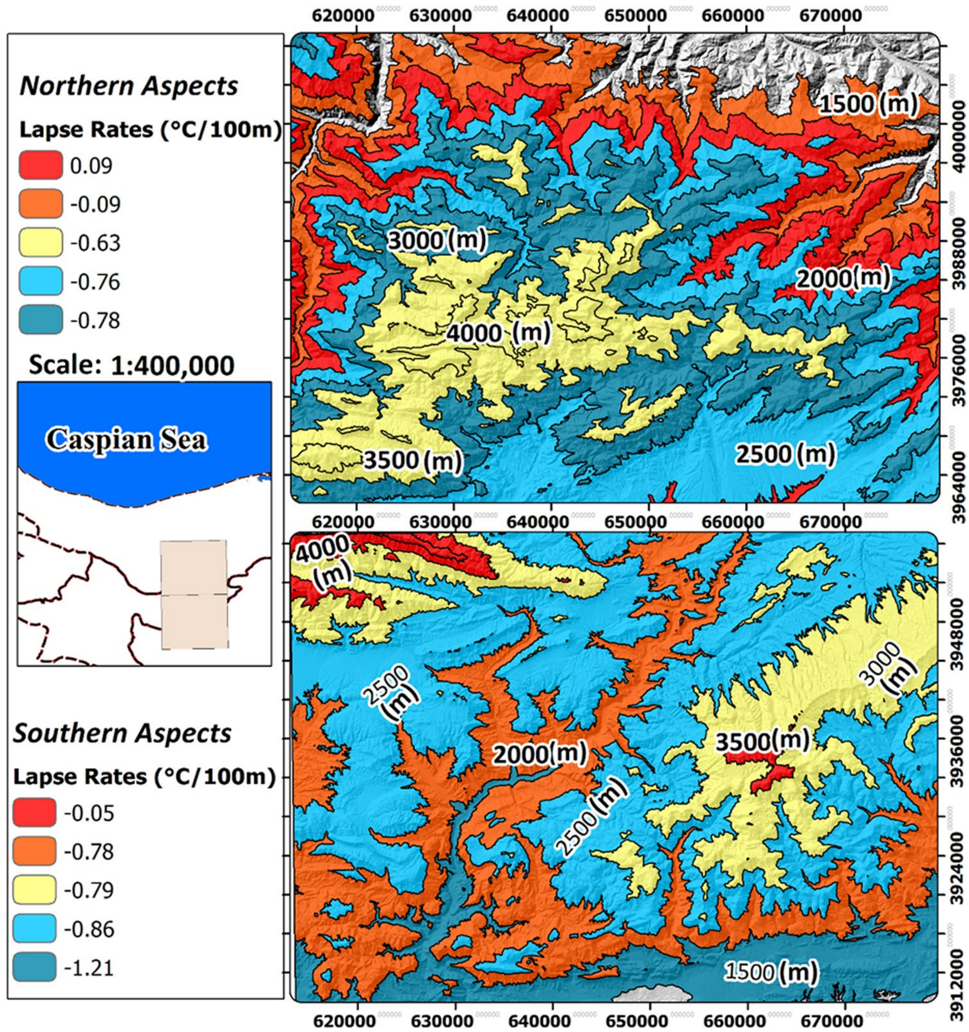

the Alborz, with the Western region having the highest (NDVI = 0.35), followed by the Eastern (NDVI = 0.28) and Middle (NDVI = 0.24) regions. In contrast, NDVI values for southern aspects range from 0.13 (Western region) to 0.09 (Eastern and Western regions).

The results showed that mean NDVI for both the northern and southern aspects of the Western region decrease with increasing elevation. The most robust vegetation cover is found at elevations between 1500 and 2000 m a.s.l. While NDVI decreases with rising elevation on the northern aspect of the Eastern and Middle Alborz, it increases with elevation on the southern aspect. Maximum and minimum NDVI values of 0.429 and 0.121 are recorded at elevations of 1000-1500 m a.s.l. and 3500-4000 m a.s.l. on the northern aspect of the Middle Alborz, while on the southern aspect, max/min NDVI values of 0.111 and 0.063 are observed at 3000-3500 m a.s.l. and 1000-1500 m a.s.l., respectively. This pattern is similar for the Eastern Alborz where max/min NDVI values of 0.483/0.205 are recorded on the northern aspect at elevations of 1500–2000 m a.s.l. and 3500–4000 m a.s.l. respectively, while on the southern aspect max/min values of 0.111 and 0.063 are recorded at 3000-3500 m a.s.l. and 1000-1500 m a.s.l. respectively. For the Western Alborz, maximum vegetation density is measured at elevations of 1500–2000 m a.s.l., for both northern (NDVI = 0.478) and southern (NDVI = 0.138) aspects, while minimum vegetation cover is observed at between 3500 and 4000 m a.s.l. (northern aspect: NDVI = 0.136; southern aspect: NDVI = 0.113) (Fig. 23).

We thus note considerable spatio-elevational variability in NDVI values across various sub-regions and slope aspects of the Alborz. A variety of factors operating synergistically may account for such findings, including differences in LST lapse rates, strength of adiabatic airflow between northern and southern aspects, variable climatic influence of the Caspian Sea, and land use patterns.

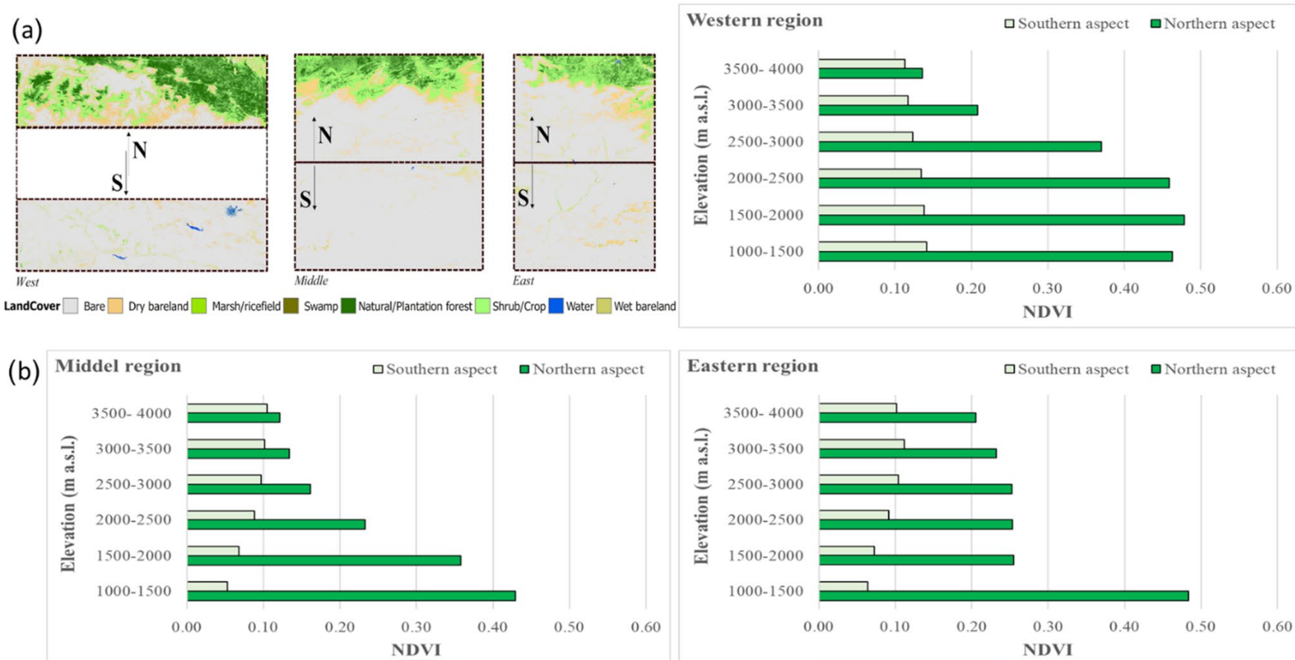

Fig. 23 **a** Land use and **b** Mean NDVI for different elevation zones (northern and southern aspects) of the three study regions, Central Alborz

4 Discussion

Our results demonstrate similar LST trends for the Eastern and Middle regions of the Central Alborz Mountains. Here, for both N and S facing aspects, LSTs have increased at all elevations during the months of January-December and June-July. In contrast, LSTs have decreased at all elevations during October, indicating an earlier onset of autumn. Although the N aspect of the Western region also records significant LST increases during January-December and June-July, such a pattern is only observed for January-December on S aspects. Instead, S aspects record significant decreasing temperatures during June-July. Such contrasting findings may, in part, be due to spatio-temporal land cover [vegetation] change across the landscape. Such an inference is supported by the work of Askarizadeh et al. (2018), who identified that decreasing vegetation cover in some parts of the Alborz has direct impact on local climate.

Similar to our findings, an earlier study (Halabian and Sehlhi 2019) focusing on the years 2003–2018, not only identified that LSTs reached maximum values during June when the sun reaches its maximum solar azimuth, but also that LSTs were substantially higher on S (as opposed to N) aspects. This is not only owing to latitudinally-controlled higher levels of insolation on S and SE aspects (Halabian and Sehlhi 2019), but also due to the climate/environmental moderating effects (increased humidity and associated increased forest cover) that the Caspian Sea has on the more directly exposed N aspects. Further, we find that annual LSTs on southern slopes increase from west to east, which is consistent with snow cover on such slopes, which decreases eastwards (Aziz, 2017). To this end, snow cover reduces air temperatures (and associated LSTs) through its albedo effect (Thiebault and Young 2020). Consequently, some of our observed LST patterns are likely influenced by topographically-controlled snow longevity. Aziz (2017) also established that snow cover had diminished most strongly in the Middle Alborz and percentage change was particularly strong above 3000 m a.s.l. This is in strong agreement with our results which indicate significant increasing LSTs on southern slopes of the Middle Alborz over December-January and at elevations over 3000 m a.s.l.

Lowest mean LSTs (14.57 °C) on N aspects are recorded for the Eastern Central Alborz region, while highest values (15.88 °C) occur in the Middle region. The Middle region also records highest mean LSTs (21.91 °C) on S aspects, while the Western region records lowest mean LSTs (18.01 °C) on this aspect. These results likely reflect the influence of local and extra-local factors. For instance, the eastern region is most strongly impacted by high pressure and cold-frontal systems that extend southwards from Siberia. This impact dissipates from east to west across the Central Alborz (Lashkari and Yarmoradi 2014; Ghangermeh et al. 2015). Western parts of the Central Alborz are also most strongly influenced by the Caspian Sea, which has temperature moderating effects (Alijani 1995). In addition, aeolian climatic influence from Turkmenistan to the northeast, has strongest climatic impact over the eastern parts of the Central Alborz (Parvin et al. 2014). Such climate influencing factors also account for strongest vegetation cover (density) over western regions, which itself has an effect on LSTs (Noroozi and Körner 2018a, b; Khare et al. 2021).

A notable finding in our study is that while LST between N and S aspects is significantly different at lower elevations (< 3000 m a.s.l.; 6.05 °C), this difference diminished with elevation, such that at 4000 m a.s.l. this difference is 1.36 °C. It seems that one of the influential factors is greater diversity in land use change for lower elevations. On the other hand, at high elevations, the variety of land use decreases and this can be effective in reducing the LST difference. However, the results of previous researches show that different slopes and elevation levels in mountainous areas experience different effects of temperature changes in the context of global warming (Pepin et al. 2015; Rottler, 2019; Pepin et al. 2022).

Our findings indicate that the impact of global warming has led to an increase in LSTs on both the N and S aspects of the Western (by 0.66 °C/decade and 0.35 °C/decade respectively) and Middle (by 0.44 °C/decade and 0.54 °C/decade respectively) regions of the Central Alborz. In strong contrast, the Eastern region of the Central Alborz records negligible LST change (0.003 °C/decade) on the N aspect and cooling (-1.01 °C/decade) on the S aspect. It is necessary to explain that various local and extra-local factors can be influential in the occurrence of such a result, and the interpretation of these changes, especially in the mountainous region, is very complex and affected by various feedbacks. At the same time, among these influential factors, it can be pointed to the change of the spatial–temporal pattern (intensification or weakening of the west–east expansion of the westerly winds or the change in the penetration and expansion of the Siberian high pressure in the east–west axis of Iran) of the atmospheric systems into the country. On the other hand, as Askarizadeh et al (2018) showed, the process of reducing vegetation changes in the recent decades in the Eastern region has expanded more intensively, which can affect the change in the temperature pattern of the area and decrease the night temperature.

LST lapse rates are considerably stronger (av = − 0.75 °C/100 m on S aspects of the Central Alborz than on the N aspect where they average − 0.36 °C/100 m. Strongest LST lapse rates on S aspects is for the Eastern region (− 0.82 °C/100 m), while that for the N aspect is for the Middle region (− 0.43 °C/100 m). Again, the moderating climatic influence of the Caspian Sea on N-facing mountain slopes facing it, as also strong vegetation cover on such slopes, (as opposed to the more arid continental-climatic and sparsely vegetated S-facing slopes), likely best explain such differences.

5 Conclusion

Studies have confirmed that global warming is having considerable consequences and threatening biodiversity in mountain regions globally (Schmeller et al. 2022). Such climate-warming related consequences on fauna and flora has also been confirmed for the Central Alborz (Fatemi et al. 2018). Our findings demonstrate strong increasing trends in LST, but also a decreasing LST anomaly on S aspects of the Eastern part of the Central Alborz. Patterns of elevational and temporal cooling/warming are thus highly complex across this mountain range and such a complexity may help better understand potentially equally complex species responses across spatial domains. Given the high elevations of the Alborz, these mountains have been a popular tourist skiing region in winter and an escape from lower elevation heat in summer (Akbarian Ronizi et al. 2016; Pourzavareh et al. 2022). Winter ski tourism is already threatened in many parts of the world due to warming and less reliable snow cover (Steiger et al. 2022). The LST trends for the Central Alborz indicate that such threats are considerable to the region, and likely to negatively impact tourism in years ahead. We anticipate that such warming will also have implications for future mountain precipitation patterns (flooding and droughts), lengthen the warm season, and have associated consequences on water resources, fire frequency and distribution, and agriculture. To this end, land use itself has impacted on the diverse nature of LST patterns in this landscape and is likely to continue doing so under continued warming scenarios.

Author contributions G.R., R.S and S.G. wrote the main manuscript text and V.N., and J.S. improve paper. All authors reviewed the manuscript.

Funding The authors have not disclosed any funding.

Declarations

Conflict of interest The authors declare no conflict of interest.

References

Akbarian Ronizi SR, Roshan GH, Negahban S (2016) Assessments of tourism climate opportunities and threats for villages located in the N coasts of Iran. Int J Environ Res 10(4):601–612

Alijani B (1995) Climate of Iran. Payam-e-Noor Publication, Payam-e-Noor. Tehran, P221 (in Persian).

Ardestani EG, Ghahfarrokhi ZH (2021) Ensembpecies distribution modeling of Salvia hydrangea under future climate change scenarios in Central Zagros Mountains. Iran Glob Ecol Conserv 26:e01488

Arsalani M, Grießinger J, Bräuning A (2022) Tree-ring-based seasonal temperature reconstructions and ecological implications of recent warming on oak forest health in the Zagros Mountains. Iran Int J Biometeorol 66:2553–2565

Asakereh H, Ashrafi S (2023) An investigation into trends in frequency and proportion of different durations of various types of extreme precipitation in Iran. Meteorol Appl 30(e2117):1–17

Askarizadeh D, Arzani H, Jafary M, Bazrafshan J, Prentice IC (2018) Surveying of the past, present, and future of vegetation changes in the central Alborz ranges in relation to climate change. J RS GIS Natural Res 9(3):1–18

Azizi G, Arsalani M, Bräuning A, Moghimi E (2013) Precipitation variations in the central Zagros Mountains (Iran) since A.D. 1840 based on oak tree rings. Palaeogeogr Palaeoclimatol Palaeoecol 386:96–103

Azizi G, Rahimi M, Mohammadi H, Khoshakhlagh F (2017) Spatio-temporal variations of snow cover in the southern slope of central Alborz. Phys Geogr Res Quart 49(3):381–393

Briscoe NJ, Morris SD, Mathewson PD, Buckley LB, Jusup M, Levy O, Maclean IMD, Pincebourde S, Riddell EA, Roberts J, Schouten R, Sears MW, Kearney MR (2022) Mechanistic forecasts of species responses to climate change: the promise of biophysical ecology. Glob Change Biol 29(6):1451–1470

Chen R, Li H, Wang X, Gou X, Yang M, Wan G (2022a) Surface air temperature changes over the Tibetan Plateau: historical evaluation and future projection based on CMIP6 models. Geosci Front 13(6):101452

Chen Z, Zhu R, Yin Z, Feng Q, Yang L, Wang L, Lu R, Fang C (2022b) Hydrological response to future climate change in a mountainous watershed in the Northeast of Tibetan Plateau. J Hydrol: Reg Stud 44:101256

Cui C, Zhang W, Hong Z, Meng L (2020) Forecasting NDVI in multiple complex areas using neural network techniques combined feature engineering. Int J Digit Earth 13(12):1733–1749

Daneshvar MR, Ebrahimi M, Nejadsoleymani H (2019) An overview of climate change in Iran: facts and statistics. Environ Syst Res 8:7

Do Nascimento ACL, Galvani E, Gobo JPA, Wollmann CA (2022) Comparison between air temperature and land surface temperature for the City of São Paulo. Brazil Atmos 13:491

Dowling TPF, Langsdale MF, Ermida SL, Wooster MJ, Merbold L, Leitner S, Trigo IF, Gluecks I, Main B, O'Shea F, Hook S, Rivera G, De Jong MC, Nguyen H, Hyll K (2022) A new East African satellite data validation station: performance of the LSA-SAF all-weather land surface temperature product over a savannah biome. ISPRS J Photogramm Remote Sens 187:240–258

Dutta D, Gupta S, Chakraborty A (2022) Effect of different land use land cover on surface heat budget: a case study from a tropical humid region of India. Remote Sens Appl: Soc Environ 25:100675

Eklundh L, Jönsson P (2016). TIMESAT for processing time-series data from satellite sensors for land surface monitoring. Multitemporal remote sensing: Methods and Applications. 177–194.

Estrada F, Kim D, Perron P (2021) Spatial variations in the warming trend and the transition to more severe weather in midlatitudes. Sci Rep. https://doi.org/10.1038/s41598-020-80701-7

Fatemi SS, Rahimi M, Tarkesh M, Ravanbakhsh H (2018) Predicting the impacts of climate change on the distribution of Juniperus excelsa M. Bieb. In the central and eastern Alborz Mountains. Iran Iforest 11:643–650

Foroozan Z, Grießinger J, Pourtahmasi K, Bräuning A (2020) 501 Years of spring precipitation history for the semi-arid Northern Iran derived from tree-ring $\delta^{18}O$ data. Atmosphere 11:889

Ghanghermeh AA, Roshan GR, Shahkooeei E (2015) Evaluation of the effect of Siberia's high-pressure extension on daily minimum temperature changes in Iran. Model Earth Syst Environ 1:20

Halabian A, Sehlhi S (2019) Investigating the relationship between snow-cover (SC) and land surface temperature (LST) with the topographic component of height in Central Alborz highlands. Quant Geomorphol Res 9(2):227–249. https://doi.org/10.22034/gmpj.2020.118243

Hill M (2013) Adaptive capacity of water governance: cases from the Alps and the Andes. Mt Res Dev 33:248–259

Huang SH, Mahmud K, Chen CJ (2022) Meaningful trend in climate time series: a discussion based on linear and smoothing techniques for drought analysis in Taiwan. Atmosphere 13:444

Huning LS, AghaKouchak A (2018) Mountain snowpack response to different levels of warming. Proc Natl Acad Sci 115(43):10932–10937

IPCC (2014) Climate Change 2014: synthesis report. Contribution of working groups I, II and III to the fifth assessment report of the intergovernmental panel on climate change. Pachauri, R., Meyer, L. (editors), Geneva, Switzerland, IPCC. ISBN: 978–92–9169–143–2

Ivanov VV (2023) Arctic sea ice loss enhances the oceanic contribution to climate change. Atmosphere 14(2):409. https://doi.org/10.3390/atmos14020409

Karimi S, Karimi S, Yavari AR, Niksokhan MH (2015) Prediction of temperature and precipitation in Damavand catchment in Iran by using LARS –WG in future. Earth Sci 4(3):95–100

Kaur A, Tanwar A, Kaur H, Singh J (2023) A study on linkage between global warming indicators and climate change expenditure. IOP Conf Ser 1110(1):012059. https://doi.org/10.1088/1755-1315/1110/1/012059

Kayet N, Pathak K, Chakrabarty A, Sahoo S (2016) Spatial impact of land use/land cover change on surface temperature distribution in Saranda Forest. Jharkhand Model Earth Syst Environ 2:127

Khare S, Latifi H, Khare S (2021) Vegetation growth analysis of Unesco world heritage Hyrcanian forests using multi-sensor optical remote sensing data. Remote Sens 13(19):3965

Körner C (2003) Alpine plant life. Springer-Verlag, Heidelberg, p 349. https://doi.org/10.1007/978-3-642-18970-8

Lashkari H, Yarmoradi Z (2014) The synoptic analysis of Siberian high-pressure situation and its paths of entrance into Iran during cold season. Phys Geogr Res Quart 46(2):199–218

Ma Q, Jin H, Wu Q, Yurova A, Liang S, Serban R, Yong-Chao L (2023) Changes in hydrological processes in the headwater area of yellow river, China during 1956–2019 under the influences of climate change, permafrost thaw and dam. Adv Clim Chang Res. https://doi.org/10.1016/j.accre.2023.03.006

Nagha S, Farid Mojtahedi N (2020) The mountains of Iran have become warmer. Hamshahri News Paper. Tehran. Iran. Article code: 92237. Accessed 09 feb 2023

Naseri E, Massah Bavani A, Sadi T (2021) Detection and attribution of changing in seasonal variability cause of climate change (Case study: hillsides of central Southern Alborz Mountains). J Sp Anal: Environ Hazards 8(1):93–110

Nasiri V, Beloiu M, Darvishsefat AA, Griess VC, Maftei C, Waser LT (2023) Mapping tree species composition in a Caspian temperate mixed forest based on spectral-temporal metrics and machine learning. Int J Appl Earth Obs Geoinf 116:103154. https://doi.org/10.1016/j.jag.2022.103154

Noroozi J, Körner C (2018a) A bioclimatic characterization of high elevation habitats in the Alborz mountains of Iran. Alp Bot 128:1–11

Noroozi J, Körner C (2018b) A bioclimatic characterization of high elevation habitats in the Alborz mountains of Iran. Alp Botany 128:1–11

Noroozi J, Pauli H, Grabherr G, Breckle SW (2011) The subnival–nival vascular plant species of Iran: a unique high-mountain flora and its threat from climate warming. Biodivers Conserv 20:1319–1338

Oko Y, Ishikawa H, Haginoya S, Ma Y (2006) Recent trends in land surface temperature on the tibetan plateau. J Clim 19:2995–3003
Overland JE, Wang M, Ballinger TJ (2018) Recent increased warming of the Alaskan marine Arctic due to midlatitude linkages. Adv Atmos Sci 35:75–84
Park T, Hashimoto H, Wang W, Thrasher B, Michaelis A, Lee T, Brosnan IG, Nemani RR (2022) What does global land climate look like at 2 degrees warming? Earth's Future. https://doi.org/10.1029/2022ef003330
Parvin G, Samaneh N, Nima FM, Hossein A (2014) Simulation of fine dust emitted from the desert of Turkmenistan to the S shores of the Caspian Sea. J Appl Res Geogr Sci 15(38):141–164
Pepin N, Bradley RS, Diaz HF, Baraer M et al (2015) mountain research Initiative EDW Working Group. Elevation-dependent warming in mountain regions of the world. Nature Clim Change 5:424–430. https://doi.org/10.1038/nclimate2563
Pepin NC, Arnone E, Gobiet A, Haslinger K, Kotlarski S, Notarnicola C et al (2022) Climate changes and their elevational patterns in the mountains of the world. Rev Geophys 60:2020000730
Pourzavareh M, Khodayari A, Kohandel M (2022) Sustainable development mountain tourism in Iran. Sports Bus J 2(2):301–320
Rottler E, Kormann C, Francke T, Bronstert A (2019) Elevation-dependent warming in the Swiss Alps 1981–2017: features, forcings and feedbacks. Int J Climatol 39(5):2556–2568
Sahani N (2021) Assessment of spatio-temporal changes of land surface temperature (LST) in kanchenjunga biosphere reserve (KBR), India using Landsat satellite image and single channel algorithm. Remote Sens Appl: Soc Environ 24:100659
Schmeller DS, Urbach D, Bates K, Catalan J, Cogălniceanu D, Fisher MC, Friesen J, Füreder L, Gaube V, Haver M, Jacobsen D, Roux GL, Lin YP, Loyau A, Machate O, Mayer A, Palomo I, Plutzar C, Sentenac H, Sommaruga R, Tiberti R, Ripple WJ (2022) Scientist's warning of threats to mountains. Sci Total Environ 853:158611
Sommer C, Malz P, Seehaus TC, Lippl S, Zemp M, Braun MH (2020) Rapid glacier retreat and downwasting throughout the European Alps in the early 21st century. Nat Commun 11(1):3209
Steiger R, Knowles N, Pöll K, Rutty M (2022) Impacts of climate change on mountain tourism: a review. J Sustain Tour. https://doi.org/10.1080/09669582.2022.2112204
Swanson DK (2021) Permafrost thaw-related slope failures in Alaska's Arctic national parks, c. 1980–2019. Permafr Periglac Process 32(3):392–406
Thiebault K, Young S (2020) Snow cover change and its relationship with land surface temperature and vegetation in northeastern North America from 2000 to 2017. Int J Remote Sens 41(21):8453–8474
Thomas J, Gupta M, Prusty G (2023) Assessing global parameters of slope stability model using earth data observations for forecasting rainfall: induced shallow landslides. J Appl Geophys 212:104994
Thompson LG, Davis ME, Thompson EM, Porter SE, Corrales GV, Shuman CA, Tucker CJ (2021) The impacts of warming on rapidly retreating high-altitude, low-latitude glaciers and ice core-derived climate records. Global Planet Change 203:103538
Vaghefi SA, Keykhai M, Jahanbakhshi F, Sheikholeslami J, Ahmadi A, Yang H, Abbaspour KC (2019) The future of extreme climate in Iran. Sci Rep 9:1464
Viviroli D, Weingartner R (2004) The hydrological significance of mountains: from regional to global scale. Hydrol Earth Syst Sci 8:1016–1029
Wang YR, Hessen DO, Samset BH, Stordal F (2022) Evaluating global and regional land warming trends in the past decades with both MODIS and ERA5-land land surface temperature data. Remote Sens Environ 280:113181
Wu S, Chao Q, Gao J, Liu L, Feng A, Deng H, Zuo L, Liu W (2023) Identification of regional pattern of climate change risk in China under different global warming targets. J Geog Sci 33(3):429–448. https://doi.org/10.1007/s11442-023-2090-1
Yan L, Roy DP (2018) Large-area gap filling of landsat reflectance Time series by spectral-angle-mapper based spatio-temporal similarity (SAMSTS). Remote Sens 10(4):609. https://doi.org/10.3390/rs10040609

Publisher's Note Springer Nature remains neutral with regard to jurisdictional claims in published maps and institutional affiliations.